

DETERMINING THE TRAJECTORY OF UNMANNED AERIAL VEHICLES BY A NOVEL APPROACH FOR THE PARTICLE FILTER

José R. G. Braga^a, Elcio H. Shiguemori^b and Haroldo F. Campos Velho^a

^a*Instituto Nacional de Pesquisas Espaciais (INPE), Av. dos Astronautas, 12227-010 São José dos Campos (SP), Brazil, jgarciabraga@gmail.com / haroldo.camposvelho@inpe.br; <http://www.inpe.br>*

^b*Instituto de Estudos Avançados (IEAv), Departamento de Ciência e Tecnologia Espacial (DCTA), Trevo Coronel Aviador José Alberto Albano do Amarante, 1 - Putim, 12228-001 São José dos Campos (SP), Brazil, elcio@ieav.cta.br; <http://www.ieav.cta.br>*

Keywords: UAV autonomous navigation, Visual odometry, Computer vision, Non-extensive particle filter.

Abstract. There are several applications of Unmanned Aerial Vehicles (UAV), such as environmental monitoring, surveillance, support to the engineering projects, entertainment, among others. The UAV autonomous navigation is one relevant research topic, and a key issue is to estimate the drone position. Here, the signal from a Global Navigation Satellite System (GNSS) is not used to estimate the UAV position. Two approaches are combined to determine the UAV positioning: a computer vision system (edge extraction in images by self-configuring supervised neural networks and correlation with geo-referenced images), and visual odometry. The two techniques are employed by a data fusion process by using a new formulation for the particle filter. The particle filter is a Bayesian method, where we are applying the Tsallis' distribution as the likelihood operator. The Tsallis' distribution has been employed to derive a generalized statistical mechanics. The filtering process is able to address the fusion data procedure, and to address the uncertainty quantification associated to the UAV trajectory estimation. The methodology was successful in performing the data fusion, generating good results and allowing to compute a confidence interval.

1 INTRODUCTION

Unmanned Aerial Vehicle (UAV) is a technology with fast development. Low cost and a variety of applications are reasons to explain the focus on this technology. Some applications include the precision agriculture (Psirofonta et al., 2017), cattle (Chamoso, 2014), environmental monitoring (Messinger and Silman, 2014), energy production (Nishar et al., 2016), surveillance (Motlagh et al., 2017), search and rescue operations (Naranjo et al., 2016), among other.

For the UAV autonomous navigation, a standard framework is to use Inertial Navigation System (INS) associated to the signal from a Global Navigation Satellite System (GNSS). However, the GNSS signal may fail. In particular, over the South America, a zone under influence of the South Atlantic Magnetic Anomaly (Cardoso, 1982), where the Earth's inner Van Allen radiation belt comes closest to the Earth's surface. Therefore, it is important to deal with a strategy without the use of the GNSS signal for UAV critical missions.

Two approaches are combined to determine the UAV positioning: a computer vision system and visual odometry. The computer vision system is based on image processing (Conte and Doherty, 2008), where the edge extraction for the UAV caught image and a geo-referenced satellite image is carried out by a self-configuring supervised neural network (Anochi et al., 2014). The correlation process from the segmented images is computed to estimate the UAV position. The data fusion from these two approaches to identify the UAV position is performed by a new Particle Filter (PF) formulation: the *non-extensive particle filter*. In this Bayesian process, the Tsallis' distribution (Tsallis, 2009) is employed as the likelihood operator. The Tsallis' distribution is derived from the maximization of the Tsallis entropy (Tsallis, 1988), a generalization of the statistical mechanics.

The filtering process is able to address the fusion data procedure. In addition, the uncertainty quantification associated to the UAV trajectory estimation is also computed by finding the confidence interval. The results obtained with non-extensive particle filter are better than those obtained using a Gaussian likelihood operation.

2 AUTONOMOUS NAVIGATION WITHOUT GNSS SIGNAL

As mentioned before, the use of a GNSS signal can fail under certain scenarios. Such issue has motivated to investigate different strategy to be employed in autonomous navigation. Two of these approaches will be described and applied to the UAV autonomous navigation.

2.1 Visual odometry

Visual odometry (VO) is a technique to estimate the vehicle position and orientation by processing the changes in the images caused by its movement (Nister et al., 2004; Scaramuzza and Friedrich, 2011) using one (monocular VO) or multiple sensors (stereo VO). Here, the monocular VO is applied to estimate the movement of outdoor UAVs. The VO basic principle is detecting interest points in the image and extract a data structure which describe them. From the interest points matching, applying the data structure, is possible to estimate the vehicle motion

For steps in sequence are necessary to execute the visual odometry:

1. *Image Sequence*,
2. *Detecting Points*,
3. *Matching between Points*,

4. Movement.

For the operation *Image Sequence*, two images caught from the sensor are up-loaded: the first image captured at instant $t - \Delta t$, and the second one at instant t . The value of Δt must be good enough for displaying the most part of the scene on both images. The *Detecting Points* operation finds the interest points in both images. For each points, a attribute vector (data structure) is build to identify it, this process is known as descriptor. One of the most successfully descriptor is the Speeded Up Robust Features (SURF) (Bay et al, 2008). The operation *Matching between Points* performs the matching between the interest points using the attribute vector. The matching is done through of a similarity metric, for example, Euclidean distance. The last step of the monocular VO algorithm, is the *Motion* estimation, which determines the movement of the vehicle using pairs of corresponding interest points. The eight point algorithm is often applied for motion estimation. This algorithm can be described by calculating the fundamental matrix F :

$$(x')^T F x = 0. \quad (1)$$

The main property of the fundamental matrix F is the correspondence condition: for a set of eight corresponding points $x \leftrightarrow x'$, there is just one matrix F satisfying equation 1. The eight point algorithm finds the fundamental matrix, and using the Singular Value Decomposition (SVD) is possible to get the vehicle motion, represented by the rotation matrix and the translation vector:

$$\text{SVD}(F) = K^T \cdot R[t]_x \cdot K^{-1} \quad (2)$$

where the K is the matrix of the intrinsic sensor parameters linked to the vehicle, R is the rotation matrix, and $[t]_x$ is the representation of the cross product of the translation vector.

2.2 Computer vision system

The image processing procedure adopted here is multi-step process – see Figure 1. Firstly, the UAV and reference images are converted to gray-scale. Secondly, a median filter is applied to the reference and UAV images to remove undesired noise (Gonzales and Wood, 2017). Edge extraction is carried out employing a supervised neural network. The multi-layer perceptron (MLP) neural network (Haykin, 1998) with back-propagation algorithm is used. An optimal architecture for a neural network is not a easy task to find. In our applications, the best neural network topology is computed as solution minimizing a functional. The optimization problem is solved by using a new meta-heuristic called *Multi-Particle Collision Algorithm* (MPCA) (Luz et al., 2008).

Multilayer perceptron

The ANN is a mathematical model, inspired by human brain processes, that tries to replicate brain behavior for solving problems. The ANN can be implemented in software or in hardware (Haykin, 1998). The MLP is a feedforward neural network, and it has been widely used. Its architecture has three main features: one input layer – composed of non-computational neurons, to receive the data from the environment –, one or more hidden layers composed of computational neurons, and one output layer composed of computational neurons.

There are two steps for the MLP training: the propagation phase, and the back-propagation phase. During the propagation phase, the input data is presented to the MLP by the input layer, and propagated up to the output layer which estimates its response $y(n)$. In this phase, the neural connection values do not change. In the back-propagation phase, the error $e(n)$ is computed by

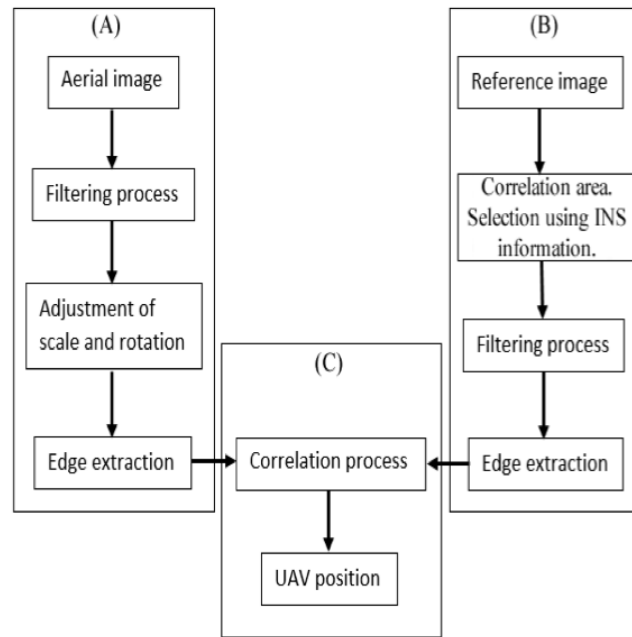


Figure 1: Sumarizing the computer vision UAV positioning system.

the square difference between the neural network response $y(n)$ and the target values, and the error $e(n)$ is back-propagated through the MLP to update the weight values. The algorithm used to up-date the weight connection values is written as

$$\Delta w(n+1) = \alpha \Delta w(n) + \eta \delta(n) y(n) \quad (3)$$

where $w(n+1) \equiv w(n) + \Delta w(n)$, α is the momentum value, η is the learning rate value, $y(n)$ is the output produced by MLP, and $\delta(n) \equiv \partial\{e(n)\}/\partial w$ is the error gradient. The number of hidden layers, the number of neurons for each layer, type of activation function, momentum, and learning rate are parameters defined by the MLP user through a process of trial and error or automatically discovered by techniques such as MPCA.

Multiple Particle Collision Algorithm (MPCA)

The MLP has been used in several applications. The MPCA is a meta-heuristic inspired in a neutron traveling inside of a nuclear reactor, where two phenomena are pronunciate: absorption, and scattering. The MPCA automatically finds the parameters that compose the ANN optimal architecture (Anochi et al., 2014) for a particular application. The MPCA is an extension of the Particle Collision Algorithm (PCA). The MPCA performs a cooperative search to find the parameter values to optimize an objective function. The objective function which determines an MLP optimal architecture is given by

$$f_{obj} = \text{penalty} \left[\frac{\rho_1 E_{train} + \rho_2 E_{gen}}{\rho_1 + \rho_2} \right] \quad (4)$$

being $\rho_1 = 1$ and $\rho_2 = 0.1$ (Luz et al., 2008) are adjustment parameters that modify the relevance attributed to E_{train} (training error) and E_{gen} (generalization error), respectively. The *penalty* is used to avoid complex architectures (high numbers of neurons) for the MLP.

3 DATA FUSION: NON-EXTENSIVE PARTICLE FILTER

The fundamental idea underlying the Sequential Monte Carlo is to represent the probability density function (PDF) by a set of samples with their associated weights. This set of samples is also referred to *particles* (Gordon, 1993). In the PF, an estimation of a *posteriori* distribution is obtained by resampling with replacement from a *priori* ensemble. As the PF does not require assumptions of linearity or Gaussianity, it is applicable to general nonlinear problems. In particular, the PF can be applied to cases in which the relationship between a state and observed data is nonlinear.

Two properties are relevant issues for the PF: the Bayes' theorem, and the Markov property. The Bayes' theorem can express by the expression to calculate the conditional probability:

$$P(A|B) = \frac{P(B|A)P(A)}{P(B)}. \quad (5)$$

The probability $P(B)$ is understood as a normalization factor. The Markov process is characterized by the property:

$$p(w_n|w_{n-1}, \dots, w_2, w_1) = p(w_n|w_{n-1}). \quad (6)$$

For the current application, the distribution w_n represents the vector with the entries being the distributions associated to the UAV position estimations computed by visual odometry and computer vision system: **the data fusion**.

The algorithm for the PF implementation can be written as:

1. Compute the initial particle ensemble:

$$\left\{ w_{0|n-1}^{(i)} \right\}_{i=0}^M \sim p_{w_0}(w_0)$$

(initial distribution $p_{w_0}(w_0)$ is a free choice: $p_{w_0}(w_0) \sim \mathcal{N}(0, 5)$);

2. Compute:

$$r_n^{(i)} = p(y_n|w_{n|n-1}) = p_{\text{et}}(y_n - h(w_n, t_n))$$

where y_n denotes observations, and:

$$\begin{aligned} p_{\text{et}}(z) &= \exp(-z^2/2)(2\pi)^{-1}; \\ z &= y_n - h(w_n, t_n) \end{aligned}$$

3. Normalize:

$$\tilde{r}_n^{(i)} = \frac{r_n^{(i)}}{\sum_{j=1}^M r_n^{(j)}};$$

4. Resampling: extract M particles, with substitution, according to (a standard notation is used here – see (Schon et al., 2005))

$$\Pr\{w_{n|n}^{(i)} = w_{n|n-1}^{(j)}\} = \tilde{q}_n^{(j)}, \quad i = 1, \dots, M;$$

5. Time up-dating: compute the new particles:

$$w_{n+1|n}^{(i)} = f(w_{n|n}^{(i)}, t_n) + \mu_n \quad \text{with: } \mu_n \in \mathcal{N}(0, 1)$$

where: $w_{n+1|n}^{(i)} \sim p(w_{n+1|n}^{(i)} | w_{n|n}^{(i)})$, $i = 1, \dots, M$;

6. Set: $t_{n+1} = t_n + \Delta t$, and go to step-2.

The kernel of the algorithm coming from the application of the Bayes' theorem and of the Markov property, suggesting the following choice:

$$\underbrace{p(w_n | Y_n)}_{\text{posteriori}_{(w_n)}} \propto \underbrace{p(y_n | w_n)}_{\text{likelihood}_{(w_n)}} \underbrace{p(w_n | Y_{n-1})}_{\text{priori}_{(w_n)}}. \quad (7)$$

Non-extensive Particle Filter

A non-extensive form of entropy has been proposed by Tsallis (Tsallis, 1988):

$$S_q(p) = \frac{k}{q-1} \left[1 - \sum_{i=1}^N p_i^q \right] \quad (8)$$

where p_i is a probability, and q is a free parameter – it is called the non-extensivity parameter. In thermodynamics, the parameter k is known as the Boltzmann's constant. Tsallis' entropy reduces to the usual Boltzmann-Gibbs-Shanon formula in the limit $q \rightarrow 1$.

As for extensive form of entropy, the equiprobability condition produces the maximum for the non-extensive entropy function, and this condition leads to special distributions (Tsallis, 2009):

$$\mathbf{q} > \mathbf{1} : \quad p_q(x) = \alpha_q^+ \left[1 - \frac{1-q}{3-q} \left(\frac{x}{\sigma} \right)^2 \right]^{-1/(q-1)} \quad (9)$$

$$\mathbf{q} = \mathbf{1} : \quad p_q(x) = \frac{1}{\sigma} \left[\frac{1}{2\pi} \right]^{1/2} e^{-(x/\sigma)^2/2} \quad (10)$$

$$\mathbf{q} < \mathbf{1} : \quad p_q(x) = \alpha_q^- \left[1 - \frac{1-q}{3-q} \left(\frac{x}{\sigma} \right)^2 \right]^{1/(q-1)} \quad (11)$$

where

$$\sigma^2 = \frac{\int_{-\infty}^{+\infty} x^2 [p_q(x)]^q dx}{\int_{-\infty}^{+\infty} [p_q(x)]^q dx},$$

$$\alpha_q^+ = \frac{1}{\sigma} \left[\frac{q-1}{\pi(3-q)} \right]^{1/2} \frac{\Gamma\left(\frac{1}{q-1}\right)}{\Gamma\left(\frac{3-q}{2(q-1)}\right)},$$

$$\alpha_q^- = \frac{1}{\sigma} \left[\frac{1-q}{\pi(3-q)} \right]^{1/2} \frac{\Gamma\left(\frac{5-3q}{2(1-q)}\right)}{\Gamma\left(\frac{2-q}{1-q}\right)}.$$

The distributions above applies if $|x| < \sigma[(3-q)/(1-q)]^{1/2}$, and $p_q(x) = 0$ otherwise. For distributions with $q < 5/3$, the standard central limit theorem applies, implying that if p_i is

written as a sum of M random independent variables, in the limit case $M \rightarrow \infty$, the probability density function for p_i in the distribution space is the normal (Gaussian) distribution. However, for $5/3 < q < 3$ the Levy-Gnedenko's central limit theorem applies, resulting for $M \rightarrow \infty$ the Lévy distribution as the probability density function for the random variable p_i . The index in such Lévy distribution is $\alpha = (3 - q)/(q - 1)$ (Tsallis, 2009).

The purpose is to use the Tsallis' thermostatics (9) or (11) for substituting the Gaussian function to represent the likelihood operator in step-2 of the PF (Campos Velho and Furtado, 2011). The idea is to explore the property of this thermostatics to access both attractors in the distribution space.

4 NUMERICAL RESULTS

The UAV images were obtained by helicopter RMAX (Yamaha Motor Company), used for testing in the Linköping University (Sweden) – see Figure 2. The helicopter flew with average speed of 3 ms^{-1} and about 60 m over the surface (altitude). The UAV camera capture images from the Nadir direction with frequency of 25 Hz. The UAV resolution is 0.12 m/pixel with 288×360 pixels, and pixel corresponds an area $\sim 1540 \text{ m}^2$. The testing trajectory has about 1 km of extension, and 1443 images/points were obtained during the test.



Figure 2: Helicopter RMAX Yamaha.

For the visual odometry, the algorithm SURF was used to identify the points of interest, and the RANSAC (RANDOM SAMple Consensus) (Fischler and Bolles, 1987) was applied to remove false corresponding points. For the computer vision system, a MLP neural network was trained to carry out the edges extraction for the objects in the images. The patterns used for image segmentation is shown in Figure 3, and Table 1 shows the MLP neural network topology determined by the MPCA optimizer.

The UAV positioning evaluation is analyzed by metrics adopted by Conte e Doherty (2008) and Braga et al. (2016) for comparison with the GPS positioning, where three metrics are employed: the Error Good Matching (EGM), the Standard Deviation Good Matching (SDGM), and Good Matching (GM). The EGM is the Euclidian distance between the estimated UAV position and that obtained by the GPS sensor on-board in the UAV. If the EGM is greater than 5 m, the estimation **is not** classified as an EGM, and it is considered an EGM otherwise. The SDGM evaluates the method stability, and it is related with the standard deviation of the UAV positioning error considering the last 30 estimation results. If the error standard deviation is greater than 2 m, the estimation **is not** considered as a SDGM. If the standard deviation is less than 2 m, the estimated trajectory is considered stable and the position is classified as a SDGM.

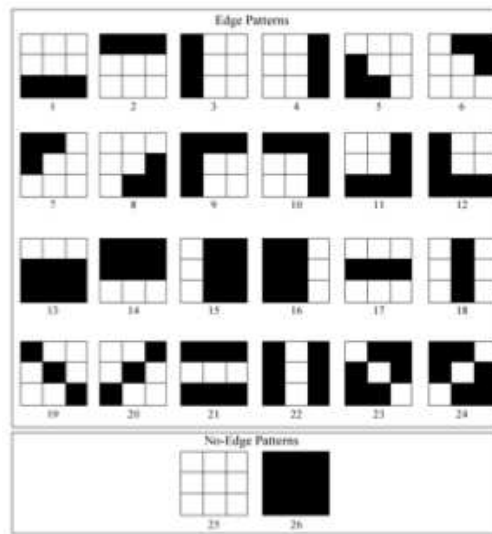


Figure 3: Patterns for MLP-NN learning phase.

If the estimated position is classified as EGM **and** SDGM, the position is a GM.

MLP-NN characters	parameter
neurons input layer	9
neurons out layer	1
number of hidden layers	1
number of neurons hidden layer	18
Activation function	tanh
Momentum	0.85
Learning rate	0.73

Table 1: Optimal topology to the MLP-NN by MPCA meta-heuristic.

For the data fusion using visual odometry and computer vision system, the nox-extensive particle filter was applied. One key issue is to select the non-extensive parameter q for our application. Here, a parametric study was performed considering 100 sampled values in the interval $q \in [0, 3]$. The initial ensemble with 1000 particles was generated with random values from a Gaussian distribution with zero mean and variance equal to one. The best value was obtained with $q = 2.57$ (Braga, 2018)).

Table 2 shows the evaluation for the UAV positioning using computer vision system (CVS), visual odometry (VO), and data fusion (CVS+VO) by non-extensive particle filter, according to the adopted metrics. The better performance was obtained with the data fusion.

Method	EGM	SDGM	GM
CVS	926	1348	856
VO	667	1413	637
NEx-PF	1381	1413	1351

Table 2: EGM, SDGM, and GM metrics for the UAV positioning experiment with different methods.

One relevant topic of research is to compute the impact of the uncertainties on the estimated

quantities. The approach dealing with Bayesian methods allows to determine the *confidence interval*, being a way to represent the uncertainty quantification. Figure 4 shows the confidence interval computed by the non-extensive particle filter used in our application.

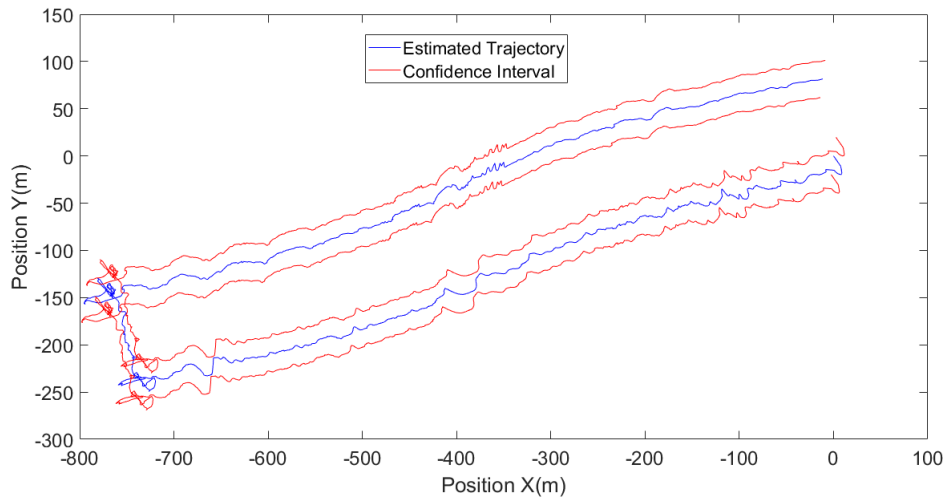


Figure 4: The confidence interval for the UAV trajectory estimated by non-extensive particle filter.

5 CONCLUSIONS

The UAV positioning by image processing was effective using visual odometry and computer vision system. The VO has a disadvantage to present a cumulative error, and CVS needs a reference marks or images to estimate the UAV position. The data fusion approach can overcome the mentioned disadvantages.

A novel approach for data fusion applied to the UAV positioning was employed and the non-extensive particle filter obtained a better estimation than standard particle filter. The method also allows to determine the confidence interval encapsulating the uncertainties linked to the present estimation problem.

ACKNOWLEDGEMENTS

Authors acknowledges to CAPES, CNPq, and FAPESP, Brazilian agencies for research support.

REFERENCES

- Anochi J. A., Campos Velho H. F., Furtado H. C. M. and Luz E. F. P. Self-configuring two types neural networks by MPCA. *2nd International Symposium on Uncertainty Quantification and Stochastic Modeling* (Uncertainties 2014), Rouen (France), 429–436, 2014.
- Braga J. R. G. *Navegação Autônoma de VANT por Imagens LiDAR*, PhD thesis, Applied Computing, National Institute for Space Research (INPE), 2018.
- Braga J. R. G., Campos Velho H. F., Conte G., Doherty P. and Shiguemori E. H. An image matching system for autonomous UAV navigation based on neural network. *14th International Conference on Control, Automation, Robotics and Vision* (ICARCV), Phuket (Thailand), 1–6, 2016.
- Bay H., Ess A., Tuytelaars T., and Gool L. V. Speeded-up robust features (SURF). *Computer Vision and Image Understanding*, 110: 346–359, 2008.

- Campos Velho, H. F. and Furtado H. C. M. Adaptive particle filter for stable distribution. In: *Integral Methods in Science and Engineering* (Eds: Christian Constanda and Paul J. Harris), 47–57, 2011.
- Cardoso A. H. Análise de alguns parâmetros ionosféricos na anomalia geomagnética do Atlântico Sul mediante ondas "VLF". *Revista Brasileira de Física*, 12: 229–246, 1982.
- Chamoso P., Raveane W., Parra V., and González A. UAVs applied to the counting and monitoring of animals. *Ambient Intelligence-Software and Applications* (Eds: Ramos C., Novais P., Nihan C., Corchado Rodríguez: *Advances in Intelligent Systems and Computing*), 71–80, 2014.
- Conte G. and Doherty P. An integrated UAV navigation system based on aerial image matching. *IEEE Aerospace Conference, Big Sky* (MT, USA), 1–10, 2008.
- Fischler M. A. and Bolles R. C. Random sample consensus: A paradigm for model fitting with applications to image analysis and automated cartography. *Communications of the ACM*, 24:381-395, 1961
- Gonzalez, R. C. and Woods, R. E. *Digital Image Processing*, 4th Edition, Pearson, 2017.
- Gordon N. J., Salmond D. J. and Smith A. F. M. Novel approach to nonlinear/non-Gaussian Bayesian state estimation. *IEE Proceedings F (Radar and Signal Processing)*, 140:107–113, 1993.
- Haykin S. *Neural Networks: A Comprehensive Foundation*, Prentice Hall, 1998.
- Luz E. F. P., Becceneri J. C., and Campos Velho H. F. A new multiparticle collision algorithm for optimization in a high performance environment. *Journal of Computational Interdisciplinary Sciences*, 1: 03–09, 2008.
- Messinger M. and Silman M. Unmanned aerial vehicles for the assessment and monitoring of environmental contamination: an example from coal ash spills. *Environmental Pollution*, 218:889–89, 2016.
- Motlagh N. H., Bagaa M. and Taleb T. UAV-based IOT platform: a crowd surveillance use case. *IEEE Communications Magazine*, 55:128–134, 2017.
- Naranjo J. E., Clavijo M., Jimeénez F., Goómez O., Rivera J. L., and Anguita M. Autonomous vehicle for surveillance missions in off-road environment. *IEEE Intelligent Vehicles Symposium*, IV:98-103, 2016.
- Nishar A., Richards S., Breen D., Robertson J. and Breen B. Thermal infra-red imaging of geothermal environments and by an unmanned aerial vehicle (UAV): a case study of the wairakei–tauhara geothermal field, Taupo, New Zealand. *Renewable Energy*, 86:1256–1264, 2015.
- Nister D., Naroditsky O. and Bergen J. Visual odometry. *IEEE Computer Society Conference on Computer Vision and Pattern Recognition (CVPR)*, Washington (DC, USA), 2004.
- Psirofonía P., Samaritakis V., Eliopoulos P. and Potamitis I. Use of unmanned aerial vehicles for agricultural applications with emphasis on crop protection: three novel case-studies. *Journal of Agricultural Science and Technology*, 5:30–39, 2017.
- Scaramuzza D. and Friedrich F. Visual odometry part I: The first 30 years and fundamentals. *IEEE Robotics and Automation Magazine*, 18:80–92, 2011.
- Schon T., Gustafsson F. and Nordlund P.-J. Marginalized particle filters for mixed linear/nonlinear state-space models. *IEEE Transactions on Signal Processing*, 53: 2279-2289, 2005.
- Tsallis C. Possible generalization of Boltzmann-Gibbs statistics. *Journal of Statistical Physics*, 52:479–487, 1988.
- Tsallis C. Nonadditive entropy and nonextensive statistical mechanics - an overview after 20 years. *Brazilian Journal of Physics*, 39:337–356, 1999.